Biosensors and Bioelectronics 136 (2019) 1–7

Contents lists available at ScienceDirect

Biosensors and Bioelectronics

journal homepage: www.elsevier.com/locate/bios

Film-Spotting chiral miniPEG-γPNA array for BRCA1 gene mutation detection

Bo Dong[a,b], Kaixuan Nie[a,b], Huanhuan Shi[a,b], Lemeng Chao[a,b], Mingyang Ma[a], Fengxiao Gao[a], Bo Liang[c], Wei Chen[d], Mengqiu Long[a], Zhengchun Liu[a,b,*]

[a] Hunan Key Laboratory for Super Microstructure and Ultrafast Process, School of Physics and Electronics, Central South University, Changsha, Hunan, 410083, PR China
[b] School of Basic Medical Science, Central South University, Changsha, Hunan, 410083, PR China
[c] State Engineering Laboratory of Highway Maintenance Technology, School of Traffic and Transportation Engineering, Changsha University of Science and Technology, Changsha, 410114, PR China
[d] Xiangya Hospital Central South University, Changsha, 410008, PR China

ARTICLE INFO

Keywords:
Peptide nucleic acid
Chiral γPNA
miniPEG
PNA array
BRCA1 mutation

ABSTRACT

Peptide nucleic acids array technology is a method of greatly increasing the throughput of laboratory processes to efficiently perform large-scale genetic tests. Diethylene glycol-containing chiral γPNA (miniPEG-γPNA) is considered to be the best PNA derivative and one of the best candidates for gene detection, because it can hybridize DNA with greater affinity and sequence selectivity than DNA and ordinary aminoethylglycyl PNA (*aeg*PNA). Herein, miniPEG-γPNA probes are synthesized by 9-fluorenylmethyloxycarbonyl (Fmoc) solid phase peptide synthesis (SPPS) in a mild condition, and a new biochip fabrication method "Film-Spotting" is invented, by which γPNA arrays with regular pattern, uniform luminance, and very low fluorescence background are obtained easily and cheaply. The miniPEG-γPNA array can effectively distinguish the full matched and mismatched targets in SSarc buffer, serum and urine, and the detection limit of complementary DNA is less than 5.97 nM. A miniPEG-γPNA array for BRCA1 gene mutation (3099delT) detection is also fabricated with a very good detection performance. This work provides an effective avenue for the diagnosis of breast cancer biomarker and expands the application of miniPEG-γPNA in the field of biochip.

1. Introduction

Since the advent of the Precision Medicine Initiative, gene detection has attracted more and more attention, and been widely applied to prenatal diagnostics (Bianchi, 2012; Vermeesch et al., 2016), cancer detection (Gao et al., 2018) and many other pathogens detection (Leigh et al., 2009; Zhang et al., 2018). Most of the established and widely used techniques for gene detection are mainly based on polymerase chain reaction (PCR) amplification and DNA sequencing techniques. These methods are laborious and costly, and require valuable instruments and special technicians. What's more, PCR is sensitive to contaminations and may sometimes introduce errors during amplification process, which will cause the decrease of detection accuracy (Gerasimova and Kolpashchikov, 2014; Mhlanga and Malmberg, 2001). Therefore, it is necessary to develop simple, rapid and portable gene detection methods for point-of-care (POC) diagnostics.

The latest statistics show that breast cancer has the highest incidence of cancer (24.2%) and the highest mortality rate (15.0%) in women all over the world (Bray et al., 2018). BRCA1 genes is a tumor suppressor gene, and mutations of this gene have been linked to hereditary breast and ovarian cancer (Prakash et al., 2015). If a woman inherits a harmful deleterious BRCA1 gene mutation, the 3099 thymine deletion (3099delT) (Kadouri et al., 2007; Thompson and Easton, 2002), the risk of getting breast cancer will be greatly increased. The early diagnosis of breast cancer is the key to increase cure incidence and survival incidence (Jafari et al., 2018; Shamsi and Islamian, 2017; Yip et al., 2018). Therefore, early and rapid detection of disease-related single nucleotide polymorphisms (SNPs) in DNA sequences associated with specific human genes has become an important topic in the field of biosensors and biochips (Bonanni et al., 2010; Chang et al., 2015; Esteban-Fernandez de Avila et al., 2015; Khoshfetrat et al., 2015).

Gene chip, also called "microarray" or "array", with DNA probes are covalently attached or physisorbed onto a proper substrate surface (slide glass, silicon substrate, gold nanoparticles, quartz, plastic tiling, nylon membranes and etc.) in array format to recognize target genes through hybridization, holds great promise in the fields of clinical

* Corresponding author. School of Basic Medical Science, Central South University, Changsha, Hunan, 410083, PR China.
E-mail address: liuzhengchunseu@126.com (Z. Liu).

https://doi.org/10.1016/j.bios.2019.04.027
Received 8 February 2019; Received in revised form 1 April 2019; Accepted 14 April 2019
Available online 19 April 2019
0956-5663/

assays and genomics because of their small volume of sample consumption, remarkably parallel and high-throughput assay capability (Ventimiglia et al., 2016). The fabrication of microarray or array mainly depends on two methods, in situ synthesis and spotting. In situ synthesis can give rise to high density microarray automatically relying on precision and expensive instruments. Spotting can produce low density spots array automatically or manually. However, automatic spotting also needs precise and expensive spotting device, and manual spotting requires complex pretreatment of the substrate to afford a substrate with hole array or hydrophilic region array. Thus, it is of great significance to develop a simple, low cost and rapid technique for the preparation of biochip.

Peptide nucleic acid (PNA) is a DNA mimic that the sugar-phosphate backbone is replaced with a neutral and achiral pseudopeptide backbone based on *N*-(2-aminoethyl)glycine units (Nielsen et al., 1991). With the synthetic polyamide neutral backbone, PNAs can hybridize to complementary DNA and RNA via Watson-Crick base-pairing with higher affinity and sequence selectivity compared with DNA (Egholm et al., 1993; Tomac et al., 1996). and hold great resistance to the degradation of proteases and nucleases (Gambacorti-Passerini et al., 1996; Nielsen et al., 1993), It makes PNA a potential candidate for gene editing (Ricciardi et al., 2018b), gene therapy (Montazersaheb et al., 2018), gene diagnosis (D'Agata et al., 2017) and other biomedical applications (Endo et al., 2005; Gupta et al., 2017).

Based on the superior hybridization ability of PNA, PNA microarray (Liu et al., 2007; Shi et al., 2015; Yang et al., 2015) has been extensively utilized for the hybridization-based gene analysis. Such as SNP and genotyping, monitoring of disease-related gene expression, pathogen detection and so on. However, the reported application of PNA microarrays or arrays are mainly based on ordinary *aeg*PNA (aminoethylglycyl PNA) probes. Many chiral PNAs have been proved to be superior to classic *aeg*PNA (Dong et al., 2016; Li et al., 2016). Insertion of only a chiral monomer to the PNA sequence has been reported to bring stronger recognition ability of DNA (Calabretta et al., 2009; Rossi et al., 2012). MiniPEG γPNA, with a relatively small, hydrophilic (*R*)-diethylene glycol ("miniPEG") unit installed at the γ-backbone can preorganize into a right-handed helix, hybridize to DNA and RNA with greater affinity and sequence selectivity, and are more water soluble and less aggregating than the parental PNA oligomers (Ricciardi et al., 2018a; Sahu et al., 2011). However, the preparation of miniPEG γPNA oligomers was based on t-butyloxy carbonyl (Boc) chemistry of solid phase peptide synthesis (SPPS), which require a strong acid condition (95% trifluoroacetic acid, TFA) to remove Boc groups in every deprotection step.

This work focus on the simple preparation and employment of a chiral miniPEG-γPNA array for the single base mutation detection in oligonucleotide sequences correlated to BRCA1 gene. Herein, chiral γPNA oligomers are prepared in a mild condition using 9-fluorenylmethyloxycarbonyl (Fmoc) protected miniPGE γPNA monomers, and γPNA arrays are fabricated with a novel and very simple method, which we call "Film Spotting". We find that the γPNA array have excellent mismatch recognition properties. A miniPEG-γPNA array for 3099delT gene mutation detection with very good performance is also prepared successfully. To the best of our knowledge, this work is the first report on the microarray based on the PNA probes containing full chiral monomers and it will expand the application of miniPEG-γPNA in the field of biochip.

2. Experimental

2.1. Materials and reagents

The ssDNAs (Table S1) were synthesized and purified by Sangon Biotech (Shanghai) Co., Ltd. (Shanghai, China). Normal human serum was purchased from AmyJet Scientific Inc, and artificial urine was from Beijing Solarbio Science & Technology Co., Ltd. Unmodified, Fmoc-protected PNA monomers were purchased from Panagene Inc. (Daejon, Korea). Fmoc-Lys(Boc)-OH, MBHA resin, and *O*-(7-azabenzotriazol-1-yl)-*N,N,N′,N′*-tetramethyluronium hexafluorophosphate (HATU) were obtained from GL Biochem (Shanghai) Ltd. (Shanghai, China). *N,N*-diisopropylethylamine (DIEA) was from Sigma-Aldrich. 3-Glycidoxypropyltrimethoxysilane (GPTS), 4,7,10-trioxa-1,13-tridecanediamine, *N,N′*-Disuccinimidyl carbonate (DSC), Trifluoroacetic acid (TFA), Trifluoromethanesulfonic acid (TFMSA), m-cresol, and thioanisole were purchased from Aladdin (Shanghai, China). *N,N*-dimethylformamide (DMF) and 1-Methyl-2-pyrrolidinone (NMP) were anhydrous grade. Dichloromethane (DCM), acetone, chloroform, acetonitrile (CAN), and other chemicals used were of analytical reagent grade. All aqueous solutions were prepared with deionized and charcoal-treated water (specific resistance $> 18.2\,M\Omega\,cm$) purified with a Milli-Q reagent grade water system (Millipore, Bedford, MA).

2.2. Synthesis of PNA oligomers

The PNA oligomers were synthesized on MBHA resin based on standard solid phase peptide synthesis (SPPS) protocols (Fields and Noble, 1990; Jaradat, 2018) with the Fmoc-protected miniPEG γPNA monomers synthesized by ourselves (Scheme S1). In brief, the MBHA resin (100 mg, 100–200 mesh, substitution of 1.1 mmol/g) was swelled for 1 h in 2 mL DMF in the reaction vessel, then drained out the solvent and washed with DMF (2mL × 2), followed by DCM (2mL × 2). Fmoc-Lys(Boc)-OH (400 μL, 0.05 mol/L, NMP), DIEA (100 μL, 0.4 mol/L, DMF), HATU (100 μL, 0.2 mol/L, DMF) were mixed together, vortexed for 10s and stood for 3min to activate the lysine monomer. The mixture was added to the resin and the reaction was continued for 1 h under agitation. Then the resins were washed with DMF (2mL × 2), followed by DCM (2mL × 2). The remaining free amines on the resins were capped with capping solution (acetic anhydride: pyridine: NMP = 1:2:2) for 30min (1.5mL × 2), then drained the capping solution and washed with DMF (2mL × 2) and DCM (2mL × 2). Next, the deprotection was realized by agitating with the solution (20% piperidine in DMF) for 5min (1.5mL × 2). After draining the deprotection solution and washing with DMF (2mL × 2) and DCM (2mL × 2), the activated Fmoc-protected γPNA monomer solution (activated in the same way for Fmoc-Lys(Boc)-OH) was added. The coupling reaction lasted 20min under agitation. Finally, the coupling solution was drained and the resin was washed with DMF (2mL × 2) and DCM (2mL × 2). A Kaiser test was performed at each step to trace coupling and double couplings were performed to guarantee a complete coupling and eliminate capping step. Deprotection and coupling of next PNA monomer were repeated as described above until the synthesis of the whole PNA probe was achieved.

Upon completion of the last monomer coupling and deprotection of the Fmoc group with deprotection solution (20% piperidine in DMF), the oligomers were cleaved from the resin and the protecting groups of nucleobases (Cbz) and side chain (methyl) were simultaneously removed after 2 h of treatment with cleavage solution (m-cresol: thioanisole: TFA: TFMSA = 1: 1: 6: 2, 2 mL). The crude mixture was eluted and precipitated in ethyl ether, dissolved in a water/acetonitrile mixture (80:20), and purified by reversed-phase HPLC (Method Info: WELCH Ultimate LB-C18 4.6 × 250 mm 5 μm; Mobile phase: A: 0.1%TFA in water, B: CAN; Flow: 1.0 mL/min; Time: 0.0–30.0min; B%: 9%–39%), and characterized by MALDI-TOF mass spectrometry, A solution of R-cyano-4-hydroxycinnamic acid (10 mg of *R*-cyano-4-hydroxycinnamic acid in 500 mL of water with 0.1% TFA and 500 mL of acetonitrile with 0.1% TFA) was used as the matrix for MALDI-TOF analysis.

2.3. Modification of slides

The following procedure was used successively to treat glass surfaces to obtain succinimidyl-functionalized glass slides (Scheme S2).

2.3.1. Epoxylation

The glass slides were treated in piranha solution (H_2SO_4: H_2O_2 = 7:3, v/v) for 1 h, rinsed with deionized water, acetone, and then dried under vacuum. The glass slides were silanized in the solution of 5% (v/v) GPTS in chloroform at 50 °C for 12 h. Sonication in chloroform was performed for 10 min to remove the noncovalently attached GPTS molecules, then the glass substrates were rinsed with acetone, and blown dry with argon.

2.3.2. Amination

The epoxylated slides were immersed in the solution of 5% (v/v) 4,7,10-trioxa-1,13-tridecanediamine in chloroform at 50 °C for 12 h, after which the slides were sonicated in chloroform for 10 min, then rinsed extensively with acetone, and finally blown dry with argon.

2.3.3. Succinimidylation

Amino-modified slides were immersed in a solution of 450 mg DSC and 1.5 ml DIEA in 50 ml acetonitrile at room temperature for 2 h, washed twice with acetonitrile and twice with dichloroethane, and dried with argon. The dried succinimidyl-functionalized glass slides were stored in argon at 2–8 °C and ready for use.

X-ray photoelectron spectroscopy (XPS) and static contact angle instrument are powerful tools for elemental composition (Nie et al., 2019; Zhao et al., 2016) and hydrophilicities of self-assembled surfaces (Li et al., 2014; Luo et al., 2019) characterization, respectively. Here these two methods were applied to characterize the modification of slides after each modification step. The detailed experimental procedure is described as the supplementary materials and the results presented in Figure S4 and Figure S5 confirm a successful modification of slides.

2.4. Fabrication and hybridization of PNA array

To obtain PNA arrays simply and cheaply, we propose a new method to fabricate a biochip, which we named it as “Film-Spotting”. The detailed procedure is shown in Scheme 1. A hole array PVC protective film was stuck onto the succinimidyl-functionalized slides to afford a microgroove array substrate. Then, the probe solutions (1 M betaine, 5 μM, 3 μL per groove) were spotted on the microgrooves of substrate directly with pipette gun, and the substrate was incubated 12 h in humidity chamber at 37 °C for probe immobilization. Next, the slide was rinsed with pure water, and deactivated in a capping solution (100 mM ethanolamine Tris buffer, pH = 9) for 30min. After capping, the slide was washed twice with 0.2%SDS solution, followed by pure water. After drying with argon, the PNA array with different probes was prepared, and ready for hybridization.

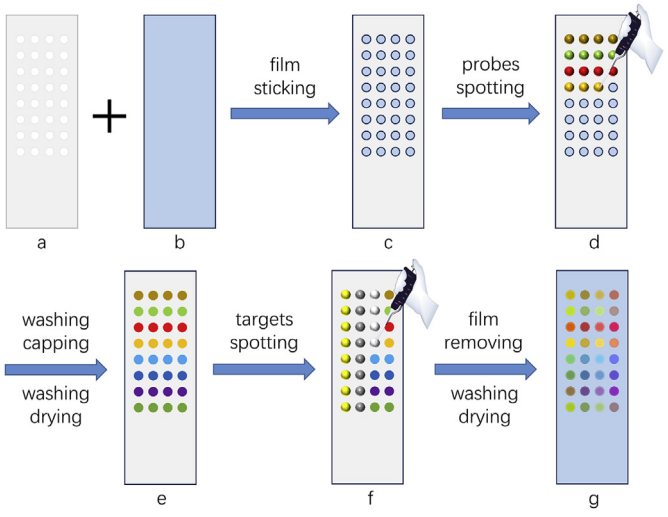

Scheme 1. Film Spotting procedure. a) Hole array protective film; b) Functionalized substrate; c) Microgroove array substrate; d) Probes are spotted on the microgroove of substrate directly; e) PNA array; f) Targets are spotted on the microgroove of substrate directly; g) PNA array hybridized with targets.

Upon fabrication of the PNA array, the target solutions (0.01–10 μM, 3 μL per groove) of 0.1 × SSarc buffer (60 mM sodium chloride, 6 mM sodium citrate, 0.72% (v/v) *N*-lauroylsarcosine sodium salt solution), serum or urine were spotted on the microgrooves of substrate directly with pipette gun, and then the chip was incubated 2 h in humidity chamber at 37 °C for hybridization. Subsequently, the PVC film was removed and the chip was washed 2 min with cleaning solution I (0.3 × SSC, 0.1%SDS), followed by cleaning solution II (0.06 × SSC), then rinsed with pure water and dried with argon.

2.5. Fluorescence signal detection

Fluorescence signal was detected on a GenePix® 4100A Scanner (Axon Instruments/Molecular Devices Corp., Union City, CA, USA), with the scan wavelength at 532 nm, PMT gain 500, Filter 575DF35, Pixel size 100 μM and Lines to average 1. The results were analyzed with the GenePix® Pro Microarray Analysis Software (Axon Instruments/Molecular Devices Corp., Union City, CA, USA).

3. Results and discussion

3.1. Characterization of PNA oligomers

Three kinds of PNA oligomers, chiral miniPEG-γPNA oligomer PNA-1, PNA-3 and achiral PNA oligomer PNA-2 were prepared (Table 1). The sequence of PNA-1 and PNA-2 chosen for this study is a model sequence, CGGACTAAGTCCATT, which was suggested by Christensen et al., (1995) to be a good test sequence, because it contains all possible coupling combinations and nearly the same composition of the four monomers, and this model sequence can prove the successful coupling reaction between different bases (Liu et al., 2007; Yang et al., 2015). And the PNA-3 was designed for the 3099delT gene mutation detection with the complementary sequence of 3099delT mutant target.

All PNA oligomers were synthesized on a solid support according to the procedure mentioned above with Fmoc chemistry, and characterized MALDI-TOF mass spectrometry (Figure S1-S3).

To confirm the conformation of PNA oligomers, we tested the CD spectra of PNA-1, PNA-2 and PNA-3 in the same concentration (Figure S6). Distinct exciton coupling patterns, with minima signal at 240 and 290 nm and maxima signal at 220 and 260 nm, characteristic of a right-handed helix were observed for PNA-1 and PNA-3, which consists well with the previous literature (Sahu et al., 2011). However, in the case of PNA-2, we did not find noticeable CD signals in the nucleobase absorption regions. The results further proved the successful preparation of the chiral γPNA probes.

3.2. Fabrication of γPNA array

To evaluate the effect of “Film-Spotting”, a γPNA array was prepared according to the above-mentioned method. A 4 × 8 holes (Φ3mm) array PVC protecting film was attached on a succinimidyl-functionalized glass slides (slowly and carefully to avoid air bubbles) to afford a 4 × 8 microgrooves array substrate. PNA-1(5 μM, dissolved in 1 M betaine, pH = 7.5) probe solution was spotted on the first two rows (spots 1–16) and blank (only 1 M betaine, pH 7.5) was spotted on the third and fourth rows (spots 17–32). After being incubated 12 h at 37 °C, cleaned and dried, the 1 μM FM target (5′-GCAATGGACTTAGT CCG -3′-TAMRA) solution was spotted on the whole array (spots 1–32) and hybridized another 2 h at 37 °C. Hybridized array was then scanned with Genepix Pro 4000A Scanner.

The results of the hybridization are shown in Fig. 1a. Obviously, an excellent PNA array with regular pattern, uniform luminance, and very

Table 1
The sequences of PNA probes[a].

Probe	Sequence (5′ to 3′)	No. of base	Calculated M	Found M
PNA-1	H-**CGGACTAAGTCCATT**-Lys-$CONH_2$	15	5958.66	5959.57
PNA-2	H-CGGACTAAGTCCATT-Lys-$CONH_2$	15	4187.71	4190.74
PNA-3	H-**TCTTACTTTAGTTTT**-Lys-$CONH_2$	15	5920.62	5923.84

[a] Bold bases indicate miniPEG-γPNA residues.

low fluorescence background was obtained by "Film-Spotting". The spots (spots 1–16) with PNA-1 probe showed a relatively strong and homogeneous fluorescence intensity (about 2500AU), and the blank spots (spots 17–32) showed an extremely weak but also similar fluorescence intensity (around 200AU). The average signal-to-noise ratio (SNR) is about 12.5:1, which means that the γPNA array can be effectively used for DNA hybridization detection.

3.3. Detection of selectivity

To investigate the validity and superiority of the γPNA array, another γPNA array was made with the same method to do some mismatch discrimination detection. Chiral γPNA probe PNA-1 (5 μM, dissolved in 1 M betaine, pH = 7.5), achiral PNA probe PNA-2 (5 μM, dissolved in 1 M betaine, pH = 7.5) and blank (only 1 M betaine, pH = 7.5) were used for comparative study. They were spotted on different line of the array (Fig. 1b, insert). For the detection of mutations, four targets were designed. Target FM with the sequence 5′-GCAATGGACTTAGTCCG-3′-TAMRA full matched to the probe target. Target MM1, 5′-GCAATGGACATAGTCCG-3′-TAMRA, with an T-A mutation was designed for single base mismatch detection. The other two targets, target MM2, 5′-GCAATGGACATAGTTCG-3′-TAMRA, and target MM3, 5′-GCAATCGACATAGTTCG-3′-TAMRA, with 2 and 3 mismatches, respectively, were also designed for the detection of multiple bases mismatches. And all four kinds of targets (2 μM, dissolved in 0.1 × SSarc buffer) were spotted on different row of the array (Fig. 1b, insert) to hybridize with different probes mentioned above.

The fluorescence scanning results of the hybridization are presented in Fig. 1b. Obvious differences were observed between the matched and mismatched target sequences hybridized to both PNA-1 and PNA-2. The fluorescence intensity ratios of PNA-1, PNA-2 and blank of the matched sequence to those of the one, two and three middle bases mismatched sequences were about 1:0.28:0.15:0.06, 1:0.45:0.32:0.15 and 1:1.03:1.02:1.03, respectively (Table S2). It showed that both the chiral γPNA probe PNA-1 and achiral PNA probe PNA-2 are able to screen single and multiple base mismatches correctly. And the ratios of 1:0.28 > 1:0.45, 1:0.15 > 1:0.32 and 1:0.06 > 1:0.15, which indicated that the mismatch discrimination performance of PNA-1 is more significant than that of PNA-2. And this result is consistent with the literature (Sahu et al., 2011). On the other hand, the fluorescence intensity ratio of full matched sequence to PNA-1, PNA-2 and blank was about 1:0.24:0.08 (Table S2), which showed that chiral γPNA probe can hybridize more easily with DNA targets than achiral PNA probe upon using same probe concentration and same target concentration, because the chiral γPNA can hybridize with DNA with better affinity and stability than achiral PNA. All the results suggested that chiral γPNA probe is superior to achiral PNA probe even when they are used in biochip. Besides, the fluorescence intensities from MM3 on both PNA-1 and PNA-2 were even lower than blank, which indicated that the labeled targets were adhered to slides by mainly the hybridization to the probes rather than physical absorption. More interesting is that a shorter miniPEG-γPNA probe can bring a better mismatch recognition result than other reported works as shown in Table 2.

3.4. Detection of sensitivity

To test the sensitivity of DNA detection by the γPNA array, a γPNA array with the PNA-1 probes (5 μM, dissolved in 1 M betaine, pH = 7.5) was prepared, and hybridized with full match DNA target FM with different concentrations of 10 μM, 5 μM, 2 μM, 1 μM, 0.5 μM, 0.2 μM, 0.1 μM, 0.01 μM and 0 (blank) in 0.1 × SSarc buffer. The results are shown in Fig. 2. The fluorescence intensities of FM target were obviously higher than the blank even in the concentration of 0.01 μM, and the fluorescence intensity increased concomitantly with the increase of target concentration (Fig. 2a). Moreover, from 0 to 2 μM, the fluorescence intensity increased significantly, and the increase of fluorescence intensity became slowly when the concentration exceeded 2 μM (Fig. 2b). This could be ascribed to the probes on the chip were free access when hybridized with 2 μM and lower concentration targets. However, once the target exceeded 2 μM, the access to probes gradually tend to be difficult due to steric hindrance from hybridized targets. There is a certain linear relationship between fluorescence intensity and target concentration from 0 to 2 μM where the regression equation is $FI = 232.987 + 3568.817C_{FM}/\mu M$ ($R^2 = 0.903$). The limit of detection (LOD) is calculated to be 5.97 nM ($C_{LOD} = 3\sigma/slope$). It shows that the γPNA array can detect DNA with high sensitivity. Considering the errors

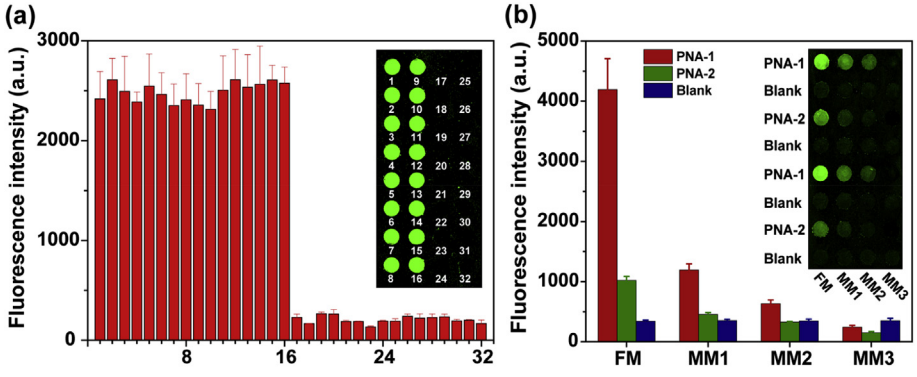

Fig. 1. Fluorescence scanning result of γPNA array. (a) Plot of fluorescence intensity of γPNA array with PNA-1 probe (spots 1–16) and blank (spots 17–32) to full matched DNA target FM, insert: hybridization fluorescence pattern; (b) Plot of the fluorescence intensity of four parallel targets (full matched target FM, single base mismatch target MM1, two base mismatch target MM2 and three base mismatch target MM3) hybridized with three probe (chiral γPNA probe PNA-1, achiral PNA probe PNA-2 and blank). The fluorescence intensity ratio of PNA-1, PNA-2 and blank of the matched sequence to those of the one, two and three middle bases mismatched sequences was about 1:0.28:0.15:0.06, 1:0.45:0.32:0.15 and 1:1.03:1.02:1.03 respectively, and the fluorescence intensity ratio of full matched sequence to PNA-1, PNA-2 and blank was about 1:0.24:0.08. insert: hybridization fluorescence pattern.

Table 2
Comparison of the detection performance of our method with other reported work.

Probe	Sequence (5′ to 3′)	No. of base	FM:MM1:MM2:MM3	Ref
aegPNA	CGTTACCTGAATCAGGC	17	1:0.37:0.25:0.11	Liu et al. (2007)
aegPNA	CGTTACCTGAATCAGGC	17	1:0.36:0.19:0.08	Yang et al. (2015)
miniPEG-γPNA	**CGGACTAAGTCCATT**	15	1:0.28:0.15:0.06	This work

from the modification of substrate and manual spotting, the γPNA array made by Film-Spotting can act as a high quality tool for the qualitative detection of DNA target because of its excellent selectivity and sensitivity.

3.5. Detection of adaptability

To evaluate the detection reliability and the application potential of the proposed γPNA array, the interferences from complex serum and urine components were investigated. Two PNA arrays were made according to the procedure described in section 3.3 and applied to hybridize with targets dissolved in serum and urine, respectively. The results are displayed in Fig. 3. Surprisingly, the mismatch discrimination ability of the miniPEG-γPNA arrays in serum and urine was even better than that in SSarc buffer. Full match and mismatch targets in the serum and urine could be distinguished clearly as the fluorescence intensity ratio of FM:MM1:MM2:MM3 was about 1:0.31:0.13:0.06 (PNA-1, serum), 1:0.43:0.27:0.19 (PNA-2, serum) 1:0.28:0.08:0.02 (PNA-1, urine) and 1:0.44:0.26:0.1 (PNA-2, urine). The fluorescence intensity ratio of full matched target to PNA-1 in different conditions (SSarc: serum: urine) was about 1:1.26:1.34 (Table S2). The results revealed that complementary DNA targets can hybridize well with γPNA arrays under physiological conditions, even if it is more complex than SSarc buffer.

3.6. 3099delT gene mutation detection

Based on the superiority of γPNA array of DNA detection, a 3099delT gene mutation detection γPNA array was fabricated. A γPNA probe PNA-3, H-**TCTTACTTTAGTTTT**-Lys-$CONH_2$, which can hybridize to the breast cancer related mutation gene, the 3099 thymine deletion (3099delT) of BRCA1 mutation, was designed, synthesized and spotted on the whole array. The wild target (5′-AAACTAAATGTAAGA-3′-TRMAR, 2 μM in 0.1 × SSarc buffer), mutant target (5′-AAAACTAAA GTAAGA-3′-TRMAR, 2 μM in 0.1 × SSarc buffer), and blank (only 0.1 × SSarc buffer) were spotted on the array according to Fig. 4a.

From Fig. 4, the scanning results were in good agreement with the expected results. Only the mutant target could bind to the chip and showed strong fluorescence intensity while the wild target and blank showed very weak fluorescence. It suggests that this γPNA array is very suitable for the 3099delT detection. A similar hybridization result was obtained when targets were dissolved in serum as shown in Figure S7 indicating further the anti-interference ability of the miniPEG-γPNA array to the complex environment in bio-samples.

4. Conclusions

In this work, miniPEG-γPNA oligomers were successfully synthesized in a mild condition using Fmoc SPPS, and a new biochip fabrication method “Film-Spotting” was invented, by which γPNA arrays with regular pattern, uniform luminance, and very low fluorescence background were obtained easily and cheaply. The hybridization results suggested that γPNA array can effectively discriminate perfectly matched and mismatched sequences in SSarc buffer, serum and urine, and chiral γPNA probe is superior to achiral PNA probe obviously. The limit of detection of miniPEG-γPNA array reached to 5.97 nM. Finally, a miniPEG-γPNA array for 3099delT gene mutation detection was prepared with a very good detection performance. This work expands the application of miniPEG γPNA in the field of biochip.

Declaration of interests

The authors declare that they have no known competing financial interests or personal relationships that could have appeared to influence the work reported in this paper.

The authors declare the following financial interests/personal relationships which may be considered as potential competing interests:

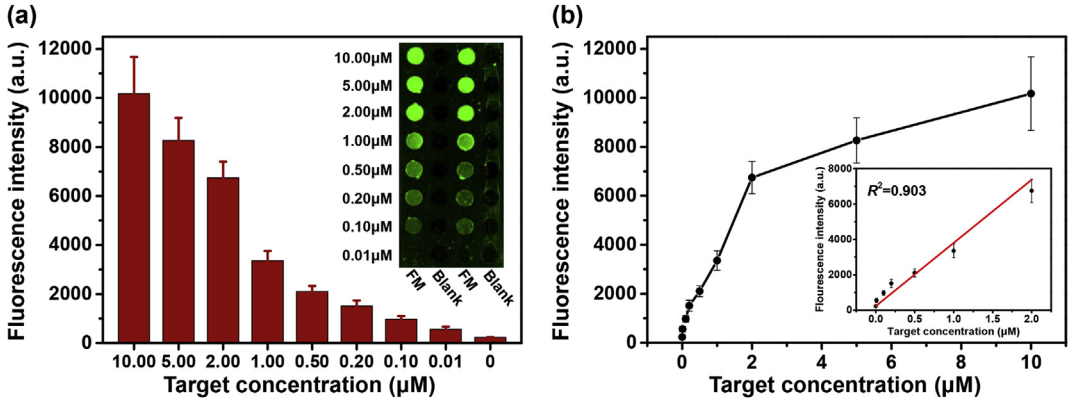

Figure 2. γPNA array hybridized with different concentrations of DNA target. (a) Plot of the fluorescence intensity of different concentrations FM targets, inset: the fluorescence scanning result; (b) the plot of the fluorescence intensity versus target concentration, inset: the calibration curve between the fluorescence intensity and target concentration range from 0 to 2 μM.

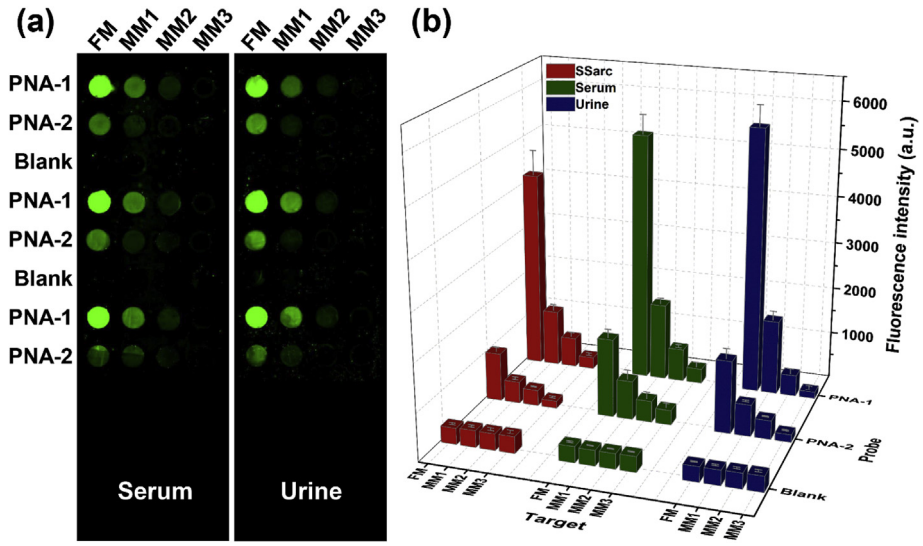

Fig. 3. DNA mismatch discrimination detection in serum and urine samples with γPNA array. (a) the fluorescence scanning result of γPNA arrays hybridized to serum and urine samples; (b) comparison of detection results under different conditions.

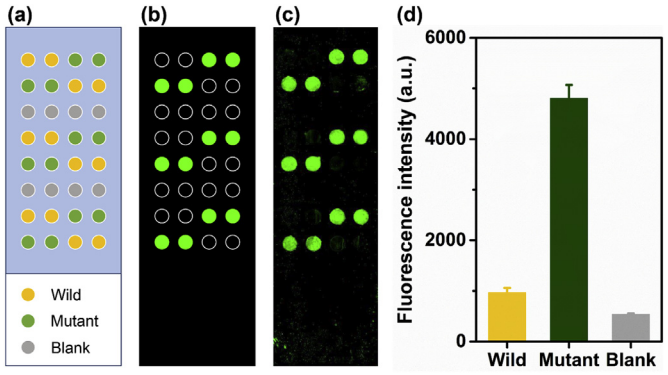

Figure 4. 3099delT gene mutation detection by γPNA array. (a) The diagram of targets spotting. Wild target (5′-AAACTAAATGTAAGA-3′-TAMAR, 2 μM in 0.1 × SSarc buffer), mutant target (5′-AAAACTAAAGTAAGA-3′-TAMAR, 2 μM in 0.1 × SSarc buffer), and blank (only 0.1 × SSarc buffer); (b) the simulated detection result; (c) the actual scanning result; (d) plot of the fluorescence intensity of three parallel targets hybridized with one probe, obtained from (c).

CRediT authorship contribution statement

Bo Dong: Conceptualization, Methodology, Investigation, Formal analysis. **Kaixuan Nie:** Investigation, Validation. **Huanhuan Shi:** Investigation, Validation. **Lemeng Chao:** Investigation, Methodology. **Mingyang Ma:** Investigation. **Fengxiao Gao:** Investigation. **Bo Liang:** Resources, Methodology. **Wei Chen:** Investigation, Resources. **Mengqiu Long:** Resources, Methodology. **Zhengchun Liu:** Conceptualization, Supervision, Resources, Writing - review & editing.

Acknowledgements

This work was supported financially by the National Natural Science Foundation of China (Grant No. 61771493, 61371042), the Natural Science Foundation of Hunan province (Grant No. 2018JJ2532), the Open-end Fund for the Valuable and Precision Instruments of Central South University (Grant No. CSUZC201825) and the Open Fund of State Engineering Laboratory of Highway Maintenance Technology (Changsha University of Science & Technology) (Grant No. KJF150104).

Appendix A. Supplementary data

Supplementary data to this article can be found online at https://doi.org/10.1016/j.bios.2019.04.027.

References

Bianchi, D.W., 2012. Nat. Med. 18, 1041–1051.
Bonanni, A., Fernandez-Cuesta, I., Borrise, X., Perez-Murano, F., Alegret, S., del Valle, M., 2010. Microchem. Acta 170 (3–4), 275–281.
Bray, F., Ferlay, J., Soerjomataram, I., Siegel, R.L., Torre, L.A., Jemal, A., 2018. Ca - Cancer J. Clin. 68 (6), 394–424.
Calabretta, A., Tedeschi, T., Di, C.G., Corradini, R., Sforza, S., Marchelli, R., 2009. Mol. Biosyst. 5 (11), 1323–1330.
Chang, K., Deng, S., Chen, M., 2015. Biosens. Bioelectron. 66, 297–307.
Christensen, L., Fitzpatrick, R., Gildea, B., Petersen, K.H., Hansen, H.F., Koch, T., Egholm, M., Buchardt, O., Nielsen, P.E., Coull, J., Berg, R.H., 1995. J. Pept. Sci. 1 (3), 175–183.
D'Agata, R., Giuffrida, M.C., Spoto, G., 2017. Molecules 22 (11), 1951–1965.
Dong, B., Nie, K., Shi, H., Li, W., Liu, Z., 2016. Curr. Org. Chem. 20 (25), 2703–2717.
Egholm, M., Buchardt, O., Christensen, L., Behrens, C., Freier, S.M., Driver, D.A., Berg, R.H., Kim, S.K., Norden, B., Nielsen, P.E., 1993. Nature 365 (6446), 566–568.
Endo, T., Kerman, K., Nagatani, N., Takamura, Y., Tamiya, E., 2005. Anal. Chem. 77 (21), 6976–6984.
Esteban-Fernandez de Avila, B., Araque, E., Campuzano, S., Pedrero, M., Dalkiran, B., Barderas, R., Villalonga, R., Kilic, E., Pingarron, J.M., 2015. Anal. Chem. 87 (4), 2290–2298.
Fields, G.B., Noble, R.L., 1990. J. Pept. Protein Res. 35 (3), 161–214.
Gambacorti-Passerini, C., Mologni, L., Bertazzoli, C., le Coutre, P., Marchesi, E., Grignani, F., Nielsen, P.E., 1996. Blood 88 (4), 1411–1417.
Gao, Y.M., Heller, S.L., Moy, L., 2018. Radiographics 38 (5), 1289–1311.
Gerasimova, Y.V., Kolpashchikov, D.M., 2014. Chem. Soc. Rev. 43 (17), 6405–6438.
Gupta, A., Mishra, A., Puri, N., 2017. J. Biotechnol. 259, 148–159.
Jafari, S.H., Saadatpour, Z., Salmaninejad, A., Momeni, F., Mokhtari, M., Nahand, J.S., Rahmati, M., Mirzaei, H., Kianmehr, M., 2018. J. Cell. Physiol. 233 (7), 5200–5213.
Jaradat, D.M.M., 2018. Amino Acids 50 (1), 39–68.
Kadouri, L., Hubert, A., Rotenberg, Y., Hamburger, T., Sagi, M., Nechushtan, C., Abeliovich, D., Peretz, T., 2007. J. Med. Genet. 44 (7), 467–471.
Khoshfetrat, S.M., Ranjbari, M., Shayan, M., Mehrgardi, M.A., Kiani, A., 2015. Anal. Chem. 87 (16), 8123–8131.
Leigh, M.W., Pittman, J.E., Carson, J.L., Ferkol, T.W., Dell, S.D., Davis, S.D., Knowles, M.R., Zariwala, M.A., 2009. Genet. Med. 11, 473–487.
Li, Q., Luo, K.H., Kang, Q.J., Chen, Q., 2014. Phys. Rev. E 90 (5), 053301.
Li, W., Shi, H., Dong, B., Nie, K., Liu, Z., He, N., 2016. Curr. Med. Chem. 23 (41), 4681–4705.
Liu, Z.C., Shin, D.S., Shokouhimehr, M., Lee, K.N., Yoo, B.W., Kim, Y.K., Lee, Y.S., 2007. Biosens. Bioelectron. 22 (12), 2891–2897.
Luo, Y., Li, Z., Zhang, W., Yan, H., Wang, Y., Li, M., Liu, Q., 2019. J. Non-Cryst. Solids 503, 214–223.
Mhlanga, M.M., Malmberg, L., 2001. Methods 25 (4), 463–471.
Montazersaheb, S., Hejazi, M.S., Nozad Charoudeh, H., 2018. Adv. Pharmaceut. Bull. 8 (4), 551–563.
Nie, K.X., Dong, B., Shi, H.H., Chao, L.M., Huang, Z.C., Long, M.Q., Xu, H., Liu, Z.C.,

Liang, B., 2019. J. Lumin. 208, 408–414.
Nielsen, P.E., Egholm, M., Berg, R.H., Buchardt, O., 1991. Science 254 (5037), 1497–1500.
Nielsen, P.E., Egholm, M., Berg, R.H., Buchardt, O., 1993. Nucleic Acids Res. 21 (2), 197–200.
Prakash, R., Zhang, Y., Feng, W.R., Jasin, M., 2015. Csh. Perspect. Biol. 7 (4), 27.
Ricciardi, A.S., Bahal, R., Farrelly, J.S., Quijano, E., Bianchi, A.H., Luks, V.L., Putman, R., Lopez-Giraldez, F., Coskun, S., Song, E., Liu, Y., Hsieh, W.-C., Ly, D.H., Stitelman, D.H., Glazer, P.M., Saltzman, W.M., 2018a. Nat. Commun. 9, 2481–2491.
Ricciardi, A.S., Quijano, E., Putman, R., Saltzman, W.M., Glazer, P.M., 2018b. Molecules 23 (3), 632–646.
Rossi, S., Calabretta, A., Tedeschi, T., Sforza, S., Arcioni, S., Baldoni, L., Corradini, R., Marchelli, R., 2012. Artif. DNA PNA XNA 3 (2), 63–72.
Sahu, B., Sacui, I., Rapireddy, S., Zanotti, K.J., Bahal, R., Armitage, B.A., Ly, D.H., 2011. J. Org. Chem. 76 (14), 5614–5627.
Shamsi, M., Islamian, J.P., 2017. Nucl. Med. Rev. Cent. E Eur. 20 (1), 45–48.
Shi, H.H., Yang, F.P., Li, W.J., Zhao, W.W., Nie, K.X., Dong, B., Liu, Z.C., 2015. Biosens. Bioelectron. 66, 481–489.
Thompson, D., Easton, D.F., 2002. Breast canc linkage, C. JNCI (J. Natl. Cancer Inst.) 94 (18), 1358–1365.
Tomac, S., Sarkar, M., Ratilainen, T., Wittung, P., Nielsen, P.E., Norden, B., Graeslund, A., 1996. J. Am. Chem. Soc. 118 (24), 5544–5552.
Ventimiglia, G., Alessi, E., Petralia, S., 2016. Sensor. Actuator. B Chem. 232, 102–106.
Vermeesch, J.R., Voet, T., Devriendt, K., 2016. Nat. Rev. Genet. 17, 643–656.
Yang, F.P., Dong, B., Nie, K.X., Shi, H.H., Wu, Y.Q., Wang, H.Y., Liu, Z.C., 2015. ACS Comb. Sci. 17 (10), 608–614.
Yip, C.H., Taib, N.A., Song, C.V., Singh, R.K.P., Agarwal, G., 2018. Curr. Breast Cancer Rep. 10 (3), 148–156.
Zhang, H.H., Liu, X.H., Liu, M.H., Gao, T., Huang, Y.Z., Liu, Y., Zeng, W.B., 2018. Biosens. Bioelectron. 99, 625–636.
Zhao, Z.W., Song, Y.X., Min, X.B., Liang, Y.J., Chai, L.Y., Shi, M.Q., 2016. J. Non-Cryst. Solids 452, 238–244.